



Supplement of

Calibration and evaluation of a broad supersaturation scanning (BS2) cloud condensation nuclei counter for rapid measurement of particle hygroscopicity and cloud condensation nuclei (CCN) activity

Najin Kim et al.

Correspondence to: Hang Su (h.su@mpic.de)

The copyright of individual parts of the supplement might differ from the article licence.

1 Supplement

2 S1. CCN activation model

3 The Activation model describes the CCNC response of transferred polydisperse charge-equilibrated particles that
4 passed through an ideal DMA. The underlying method is similar to Petters et al. (2007), but the calculation part
5 of CCN activation fraction is modified for the BS2-CCN system. Here, we summarize procedure and relevant
6 equations.

7 DMA classifies particles with a narrow range of electrical mobilities. The electrical mobility, Z_p , is defined in Eq.
8 (S1) to determine the particle size associated with the range of mobilities.

$$9 \quad Z_p = \frac{neC}{3\pi\mu D_p} \quad (S1)$$

10 where e is the elementary charge, C is the Cunningham slip correction, μ is the dynamic viscosity of air and n is
11 the number of elementary charges on the particle. The relationship between particle electrical mobility (Z_p^*) and
12 DMA parameters are defined by Knutson and Whitby (1975). The relationship is given in Eq. (S2).

$$13 \quad Z_p^* = \frac{Q_{sh}}{2\pi LV} \ln \left[\frac{R_2}{R_1} \right] \quad (S2)$$

14 The mobility bandwidth, Z_p , is:

$$15 \quad \Delta Z_p = \frac{Q_a}{Q_{sh}} Z_p^* \quad (S3)$$

16 where Q_{sh} , and Q_a are the volumetric sheath flow and aerosol flow, respectively. L is the length of the DMA
17 column, V is the negative potential applied to the inner cylinder. R_1 and R_2 are the inner and outer radius of the
18 annular space of DMA, respectively. The transfer function for a cylindrical DMA column, $\Lambda(Z)$, is a piecewise
19 linear probability function of triangular shape which is $\Lambda(Z_p^*) = 1$, $\Lambda(Z_p^* - 0.5\Delta Z_p) = \Lambda(Z_p^* + 0.5\Delta Z_p)$, and
20 $\Lambda(Z_p^* - \Delta Z_p) = \Lambda(Z_p^* + \Delta Z_p) = 0$.

21 The fraction of particles carrying n charges (+1, +2) at charge equilibrium, $f(D, n)$, is calculated based on
22 Wiedensohler (1988).

$$23 \quad \log_{10}[f(D, n = +1, +2)] = \sum_{i=0}^5 a_i(n)(\log_{10}D)^i \quad (S4)$$

24 where $a_i(n)$ are coefficients obtained from DMA (TSI 3081) manual. As the size range of the particles covered
25 in this study is less than 300nm, the fraction of particles carrying three or more charges is excluded.

26 With an assumed particle size distribution, an idealized CCN instrument response is determined by the following
27 procedures. N_{CN} at D_{Z^*} can be calculated using Eq. (S5). Equation (8) is for transforming the particle size
28 distribution, dN/dD into the mobility domain.

$$29 \quad N_{CN}(D_{Z^*}) = \sum_{n=1}^2 \left[\int_{Z=Z^*+\Delta Z}^{Z=Z^*-\Delta Z} f(D_{Z,n}, n) \Lambda(Z) \frac{dN_n}{dZ} dZ \right] \quad (S5)$$

$$30 \quad \frac{dN_n}{dZ} = \frac{dD}{dZ} \frac{dN}{dD} \quad (S6)$$

31 where, dN_n/dZ is the differential size distribution of +n-charged particles in the mobility domain. It is noted that
 32 electrical mobility Z^* is based on a particle with +1 charge ($D_{Z^*,1}$), which should be assumed to define $\Lambda(Z)$.
 33 Similar to the N_{CCN} , the number of particles that activate as CCN is calculated as follows:

$$34 \quad N_{CCN}(D_{Z^*}) = \sum_{n=1}^2 \left[\int_{Z=Z^*+\Delta Z}^{Z=Z^*-\Delta Z} h(D_{Z,n}) f(D_{Z,n}, n) \Lambda(Z) \frac{dN_n}{dZ} dZ \right] \quad (S7)$$

35 where $h(D_{Z,n})$ is a function for a fraction of particles that activate as cloud droplets. For the BS2-CCN system,
 36 the activation fraction, $h(D_{Z,n})$, is calculated by Eq. (S8) and (S9). The activation fraction of aerosol particles
 37 with the same $S_{aerosol}(D_{Z,n})$ is calculated by integrating the activation fraction function $g(x)$ and flow velocity
 38 $v(r)$ over the cross-section of the aerosol flow (Su et al., 2016). This is calculated as follows:

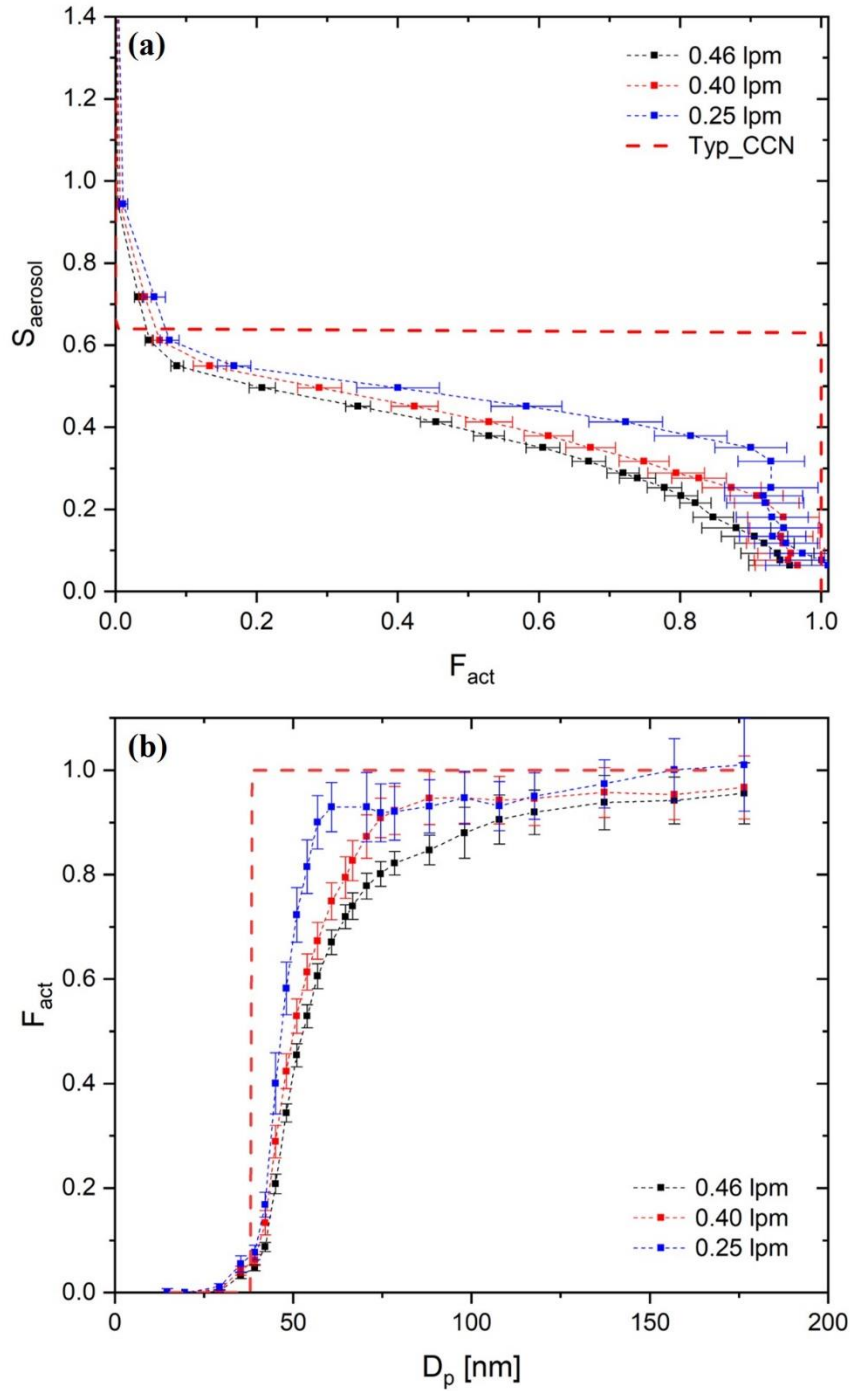
$$39 \quad h(D_{Z,n}) = \frac{2\pi \int_0^r v g(S_{aerosol}(D_{Z,n}) - S_{tube}(r)) r dr}{2\pi \int_0^r v r dr} \quad (S8)$$

$$40 \quad g(x) = \begin{cases} 1 & \text{if } x \leq 0 \\ 0 & \text{if } x > 0 \end{cases} \quad (S9)$$

41 Where r is the radial distance to the centerline of the activation unit (i.e., $r = 0$ for the center). $S_{tube}(r)$ is a
 42 typical distribution of supersaturation in the activation tube of CCNC and can be calculated as $S_{tube}(r) =$
 43 $S_{max} \times \cos(0.14 \times r)$. The S_{tube} profile is adopted from [http://nenes.eas.gatech.edu/Experiments/CFSTGC.](http://nenes.eas.gatech.edu/Experiments/CFSTGC.html)
 44 [html](http://nenes.eas.gatech.edu/Experiments/CFSTGC.html). It is noted that the unit of S is %, and the unit of r is millimeters. Although $S_{tube}(r)$ in the activation tube
 45 is also dependent on an axial (Robert and Nenes, 2005), $S_{tube}(r)$ in this study simply represent the maximum S
 46 in the axial direction at a given r . Flow velocity is prescribed as $v(r) = v_m \times (1 - r^2/R^2)$, where v_m is the
 47 maximum velocity at the centerline of the activation unit. It is noted that specific $S_{aerosol}(D_{Z,n})$ corresponding to
 48 each D_{Z^*} of a known particle can be calculated by Eq. (2) In this study, we used ammonium sulfate as calibration
 49 aerosols and set 0.63% for S_{max} .

50

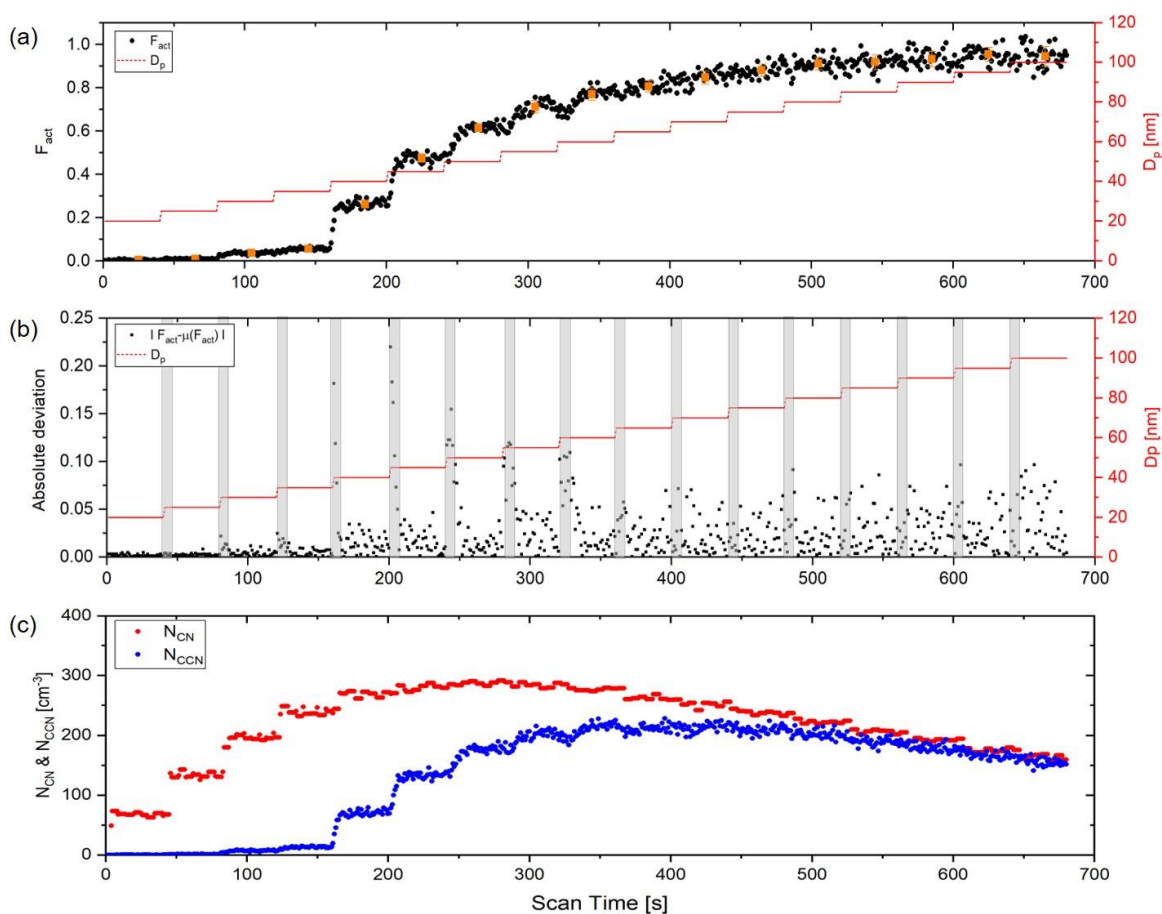
51



52

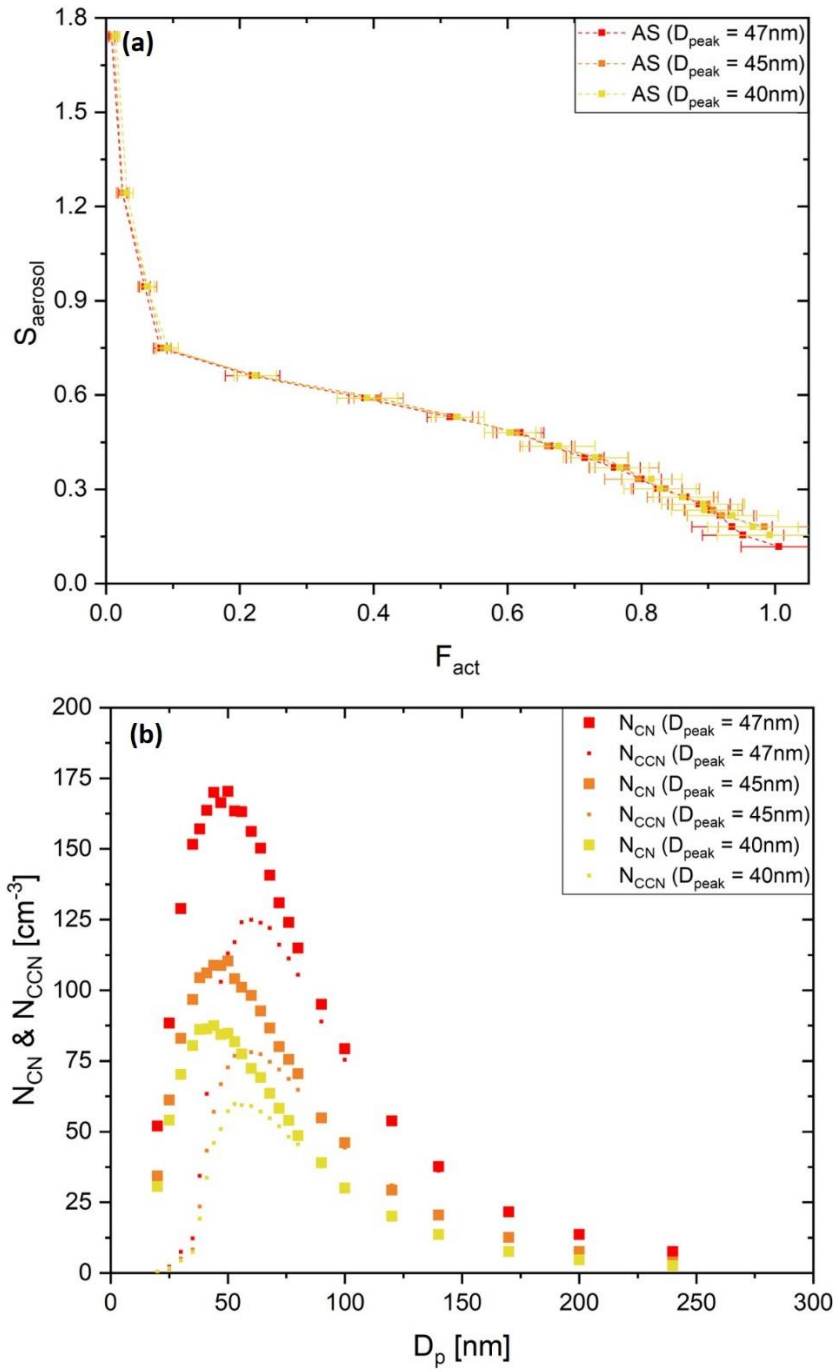
53 **Figure S1: (a) Calibration curves ($F_{act} - S_{aerosol}$) and (b) activation curve ($F_{act} - D_p$) for three different sample**
 54 **flows (0.46 lpm (black), 0.40 lpm (red) and 0.25 lpm (blue)). Red dashed line indicates an ideal result of typical CCNC**
 55 **for comparison. Total flow (sample + sheath) is set to be 0.50 lpm. The experiment is conducted under $dT=8$ K setting**
 56 **with ammonium sulfate particles.**

57



58

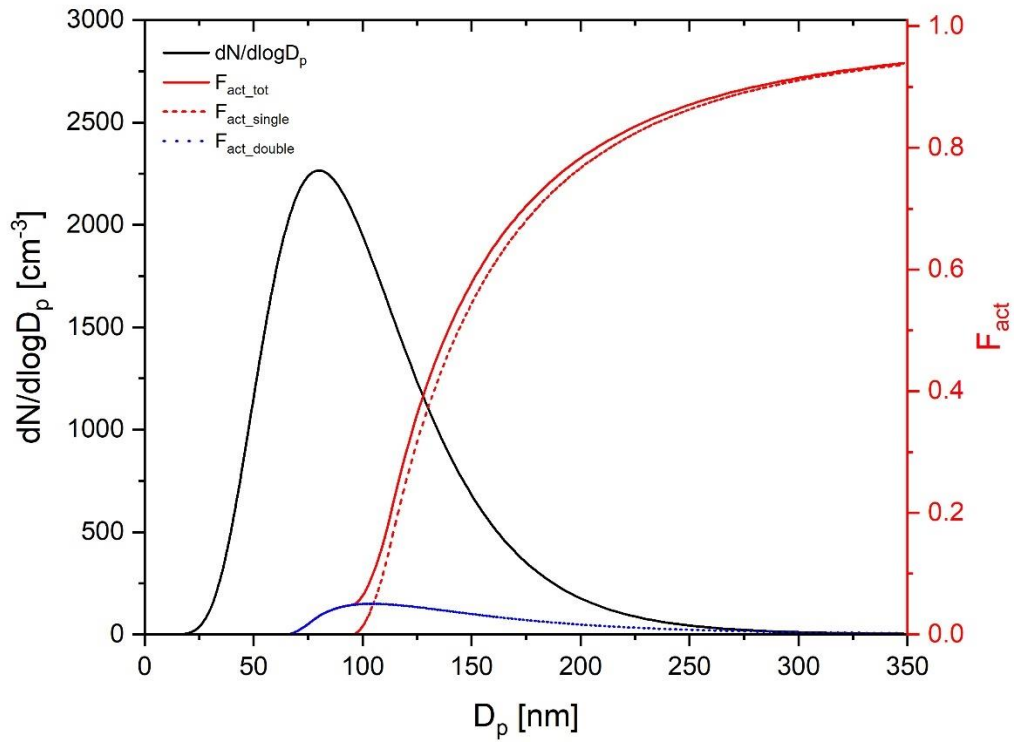
59 **Figure S 2: Exemplary D_p scan (20-100 nm) of lab generated ammonium sulfate. (a) 1 second data of activated fraction**
 60 **(F_{act}), marked in black dot (left ordinate), particle diameter (red line, right ordinate). Average and standard deviation**
 61 **of each diameter (30-second average data except for 10 seconds of stabilization) are presented in orange square with**
 62 **bar. (b) Absolute deviation of F_{act} (black dot, left ordinate) and particle diameter (red line, right ordinate): The grey**
 63 **shaded box indicates the stabilization time (~10 seconds) of each particle diameter. (c) Particle number concentration**
 64 **(N_{CN} , red dot) and CCN number concentration (N_{CCN} , blue dot). Time resolution of each data point is 1 second and**
 65 **the particle diameter is changed every 40 seconds. S_{max} is set to be 10 K (0.8%).**



66

67 **Figure S3: (a) Calibration curves and (b) number size distributions of N_{CN} and N_{CCN} of ammonium sulfate particle**
 68 **for $dT=10\text{ K}$.**

69

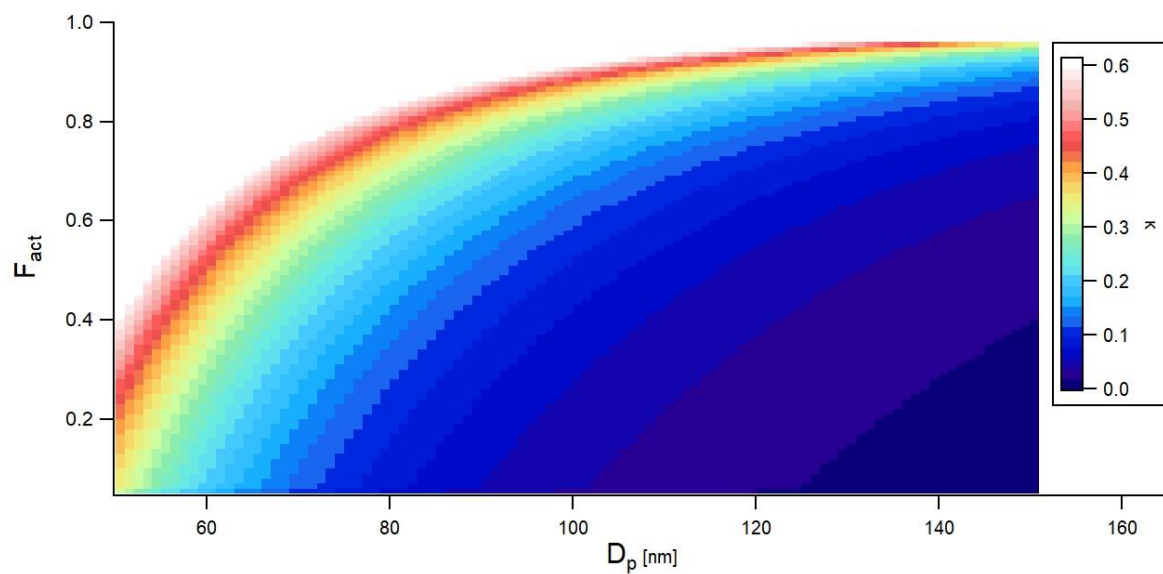


70

71 **Figure S 4: Calculated ideal activation fraction for log-normally distributed, charge-equilibrated particles transmitted**
 72 **BS2-CCNC system Shown are assumed particle size distribution (black-solid line, left ordinate, $N =$**
 73 **1000 cm^{-3} , $D_g = 80 \text{ nm}$, and $\sigma_g = 1.5$, total activation fraction (red solid line), activation fractions by singly**
 74 **charged particle (red dashed line) and doubly charged particle (blue dashed line). It is noted that S_{max} is set to be 0.2%**
 75 **in this calculation.**

76

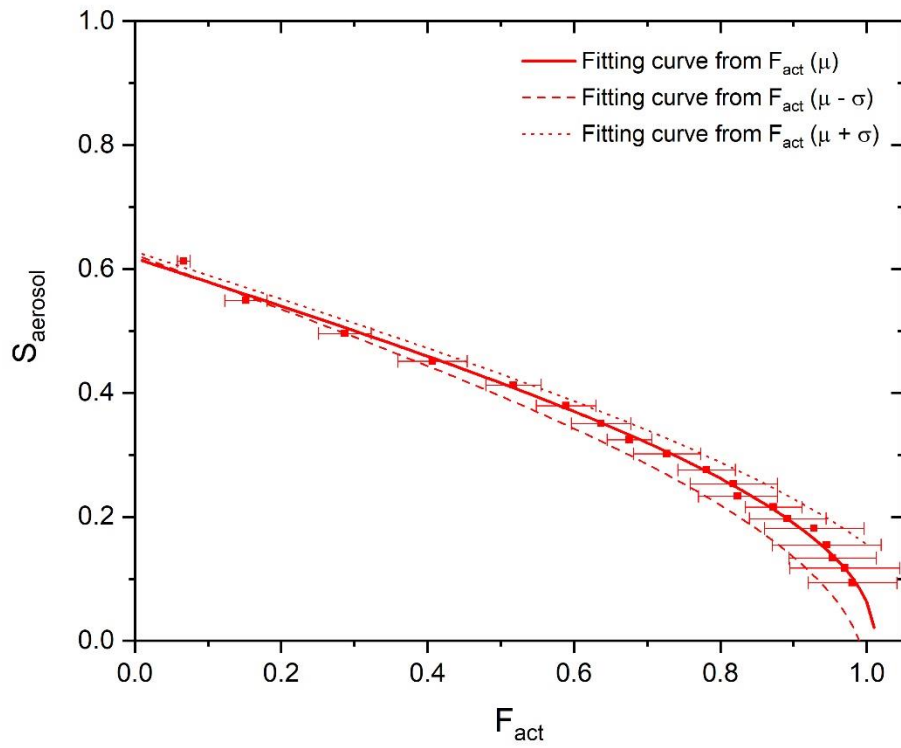
77



78

79 **Figure S5: κ distribution which corresponds to the F_{act} values of a particle ranged from 50 nm to 150 nm. It is**
 80 **calculated from the fitting curve (Eq.3) of $F_{act} - S_{aerosol}$ relation for $dT=8$ K condition. Details of the fitting curve**
 81 **equation are described in Section 2.4, and the coefficients of the equation are presented in Table 1.**

82



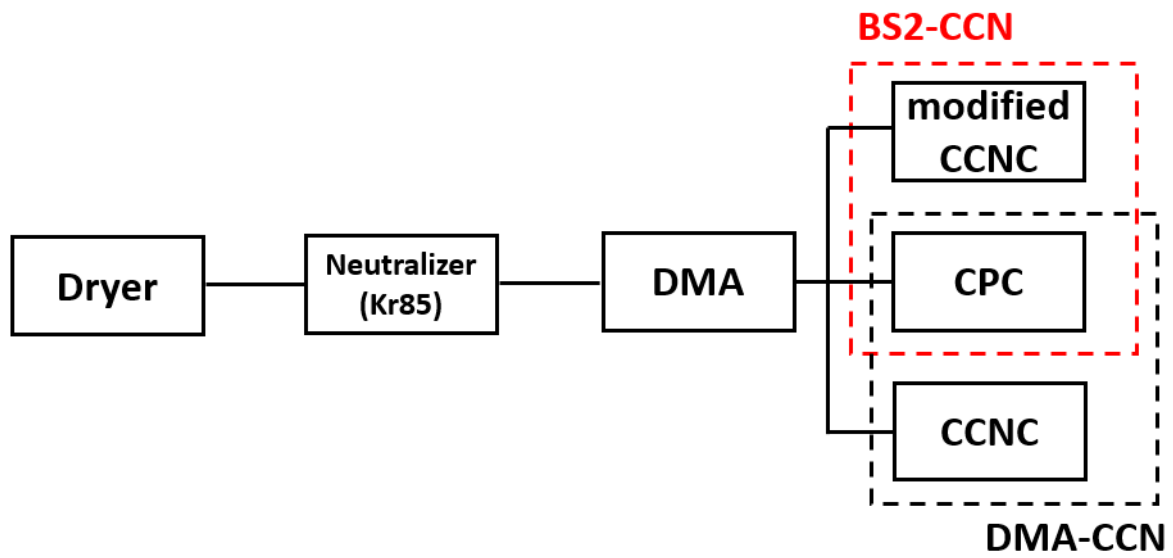
83

84 **Figure S 6: Experimental data point (square dot with error bar) and fitting curves for $dT=8$ K ($S=0.63\%$) condition.**

85 **Solid line is obtained from data of $F_{\text{act}} (\mu)$. Dotted and dashed fitted line are obtained from data of $F_{\text{act_high}} (\mu + \sigma)$**

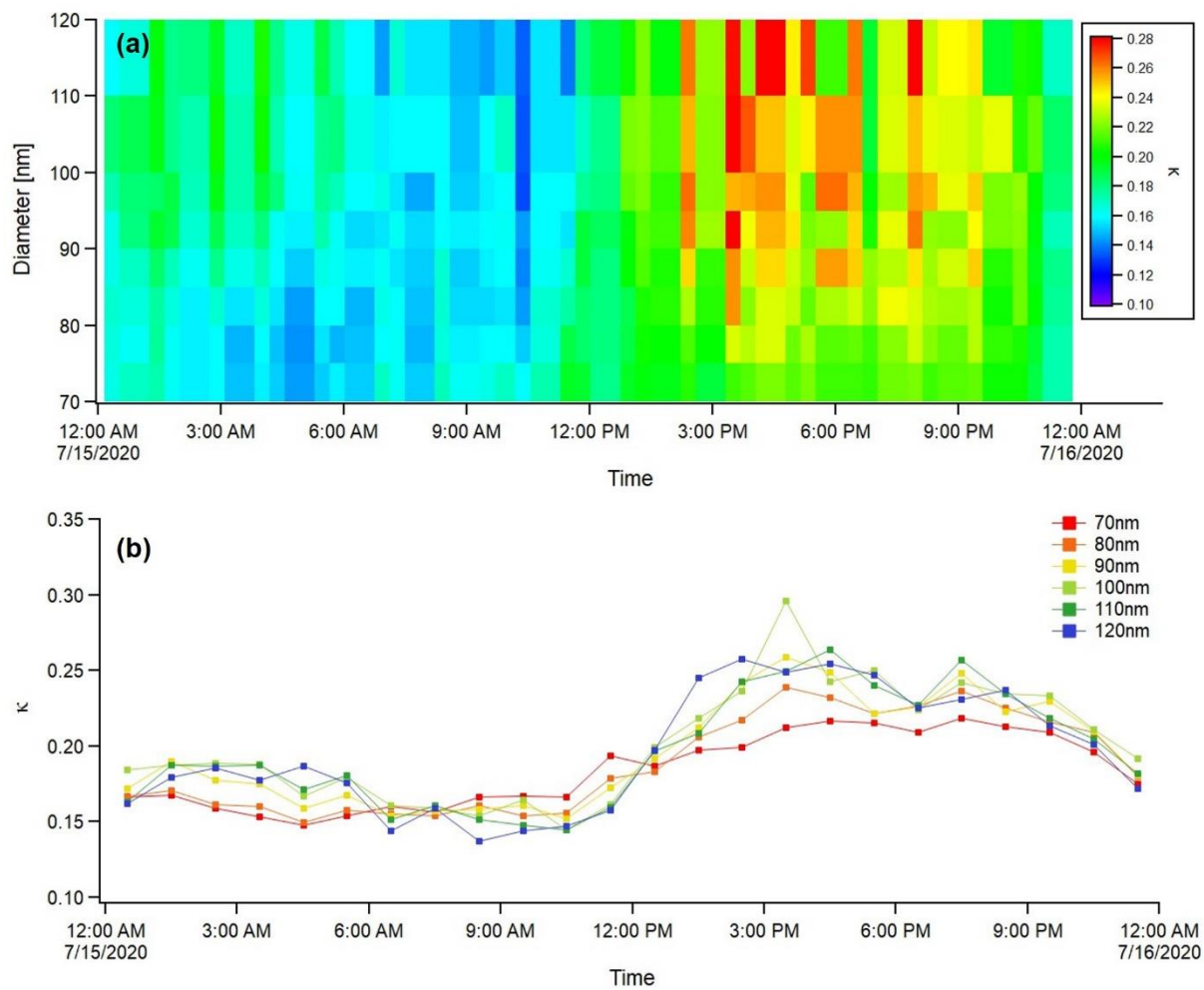
86 **and $F_{\text{act_low}} (\mu - \sigma)$. μ and σ indicate average and standard deviation of F_{act} , respectively.**

87



88

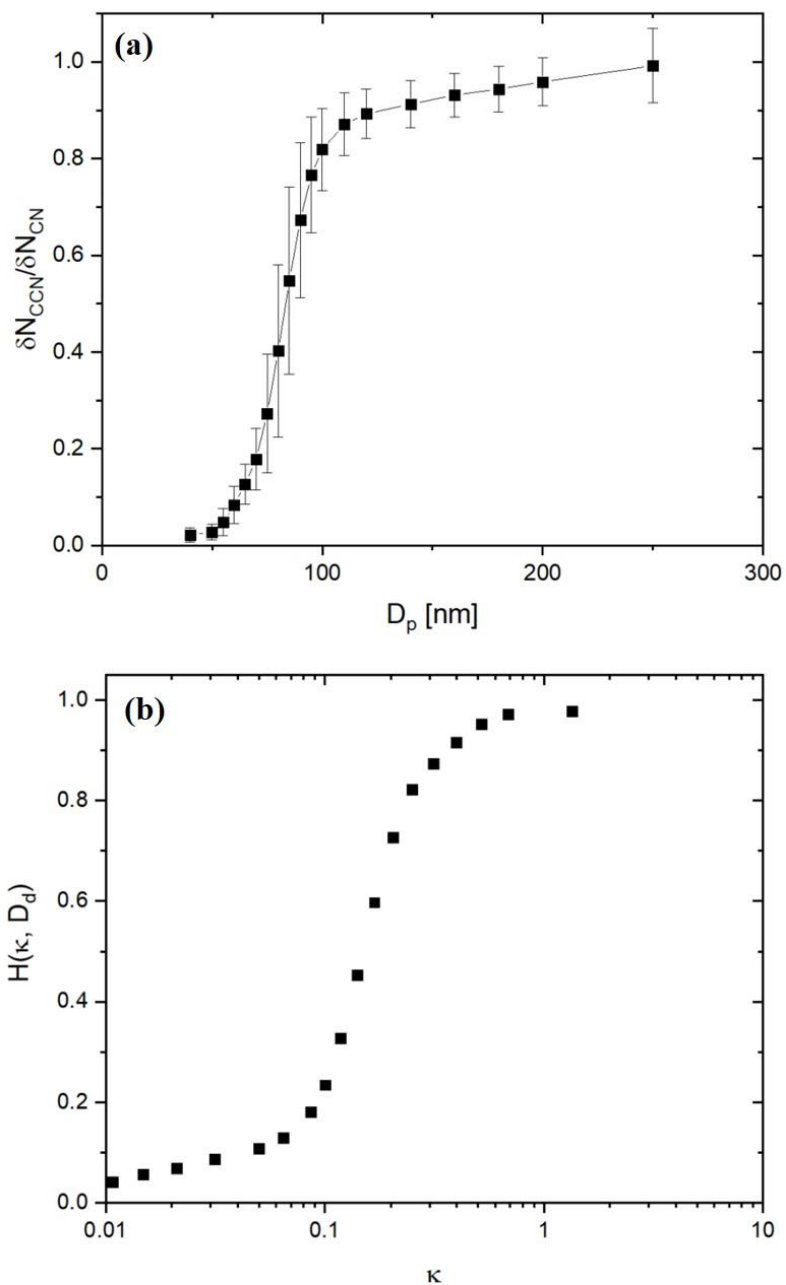
89 **Figure S7: Schematic plot of instrumental setup for inter-comparison between DMA-CCN and BS2-CCN**
 90 **measurement**



91

92 **Figure S8: Diurnal variation of (a) κ distribution and (b) κ value of each D_p (between 70 nm and 120 nm) during the**

93 **intercomparison experiment for ambient aerosols.**



94

95 **Figure S9: (a) Average CCN efficiency spectra and (b) average cumulative particle hygroscopicity distribution,**
 96 **$H(\kappa, D_d)$, of DMA-CCN measurement for 0.4% S. The $H(\kappa, D_d)$ value in panel (b) refers to different sizes. $H(\kappa, D_d)$ is**
 97 **defined as the number fraction of particles having a hygroscopicity parameter smaller than κ at a given dry diameter,**
 98 **D_d (Su et al., 2010).**